

DIRECT OBSERVATION OF THE GROWTH OF VOIDS IN
MULTIFILAMENTARY SUPERCONDUCTING MATERIALS VIA HOT
STAGE SCANNING ELECTRON MICROSCOPY*

J. Ling-Fai Wang

John T. Holthuis

Milton R. Pickus

Richard W. Lindberg

NOTICE

This report was prepared as an account of work sponsored by the United States Government. Neither the United States nor the United States Department of Energy, nor any of their employees, nor any of their contractors, subcontractors, or their employees, makes any warranty, express or implied, or assumes any legal liability or responsibility for the accuracy, completeness, or usefulness of any information, apparatus, product, or process disclosed, or represents that its use would not infringe privately owned rights.

*This work was supported by the Division of Materials Sciences,
Office of Basic Energy Sciences, U. S. Department of Energy,
under contract No. W-7405-Eng-48.

DIRECT OBSERVATION OF THE GROWTH OF VOIDS IN
MULTIFILAMENTARY SUPERCONDUCTING MATERIALS VIA HOT
STAGE SCANNING ELECTRON MICROSCOPY

J. LING-FAI WANG

JOHN T. HOLTHUIS

MILTON R. PICKUS

Materials and Molecular Research Division

Lawrence Berkeley Laboratory

University of California

Berkeley, California 94720

RICHARD W. LINDBERG

Engineering and Technical Services Division

Lawrence Berkeley Laboratory

University of California

Berkeley, California 94720

Key Words: SEM, Hot Stage, Voids, Multifilamentary Superconductor,
Diffusion.

ABSTRACT

The need for large high field magnetic devices has focused attention on multifilamentary superconductors based on A15 compounds such as Nb_3Sn . The commercial bronze process for fabricating multifilamentary superconducting Nb_3Sn wires has been developed to a high degree of sophistication. A major problem in their application is their strain sensitivity when long reaction times are employed. There is a need to determine the fundamental causes for the degraded mechanical and superconducting behavior.

An improved hot stage for the scanning electron microscope has been constructed to study the formation of the A15 phase by solid state diffusion. The nucleation and growth of voids near the interface of the A15 phase (Nb_3Sn) and matrix (bronze) were observed and monitored directly and recorded on video tape. Successive layers of material heated in the hot stage were subsequently removed and the new surfaces were re-examined, using SEM-EDX and optical microscopy, to confirm the fact that the observed porosity was indeed a bulk rather than a surface phenomenon. These voids are considered to be a primary cause for degrading the mechanical, thermal and superconducting properties.

INTRODUCTION

Modern technology has placed increasing demands on materials. This need for better materials is particularly acute in the area of superconductors. It is now widely recognized that for advanced energy research and technology, such as magnetic fusion and high energy physics, a need exists for multifilamentary superconductors with high critical fields and critical temperatures. The most promising candidates are the A15 compounds such as Nb_3Sn . All of these compounds are brittle and, therefore, difficult to obtain in the required form.

Conductors based on the reduction of composites of Nb-Ti alloy rods in a copper matrix have been developed commercially to a high degree of sophistication. These conductors have a series of advantages that are very important in the utilization of superconducting materials. They include the combination of the following properties:

1. high electrical and thermal conductivity;
2. excellent reproducibility of properties;
3. excellent ductility which facilitates (a) design, (b) manufacture, (c) shaping and forming;
4. filament and matrix mutually nonreactive.

The limitation is that this Nb-Ti superconductor has $T_c = 10^\circ K$, $H_c = 120KG$.

The technology for fabricating Nb-Ti multifilamentary superconductors has been successfully transferred to manufacture multifilamentary superconductors based on the compound Nb_3Sn . Niobium rods are inserted into a Cu-13%Sn bronze matrix. The composite is then reduced to wire form. By solid state diffusion reaction, the compound Nb_3Sn is formed at the interface between the Nb filaments and the bronze matrix. This is the so-called bronze process. Unfortunately, the strain sensitivity and

thermal instability of these conductors have been recognized recently and constitute potentially major problems in their application¹.

There is a need to determine the fundamental causes for the resulting degradation of the mechanical and superconducting properties of bronze process wire. During the past year, D. S. Easton and D. M. Kroeger² reported the observation of Kirkendall voids revealed by their room temperature microscopy work on reacted samples. There is skepticism in the superconducting community in regard to the actuality of the existence of these voids and, therefore, to the significance of their role.

In the bronze process wire, each niobium filament forms a diffusion couple with the bronze matrix. The rate of diffusion of each metal into the other is different. Across the interface that separates the two metals there is a greater amount of mass transport in one direction. Consequently, the material into which the faster diffusing species moves will expand and the other will contract. Also because there is an opposite flow of vacancies the side losing material (in this case the bronze matrix) will have an excess of vacancies. This diffusion phenomenon is similar to the Kirkendall effect³ and can lead to void formation. When the Kirkendall effect takes place, stresses are also created. The side gaining material is put in compression, and the side losing material in tension.

It was determined that there is an urgent need to carry out a basic research program not only to confirm the existence of the Kirkendall voids in superconducting materials fabricated from niobium rods arrayed in a bronze matrix but also to confirm their circumvention in

other approaches, such as LBL's infiltration process. This report will deal mainly with the confirmation of the existence of voids in reacted bronze process wire.

Room temperature microscopy on reacted samples was carried out at LBL. As the reaction time increased the reacted product became very brittle. Although the micrographs show an increase in the number and size of voids as a function of reaction time, the brittleness of the reacted products makes it difficult to distinguish the voids created by the not-so-perfect polishing techniques. This prompted us to develop a program to do an in-situ study of the diffusion reactions, using a scanning electron microscope with an improved hot stage.

EXPERIMENTAL

The details of the development of a scanning electron microscope hot stage have been described previously by R. M. Fulrath⁴ and D. N. K. Wang, et al⁵. We have constructed a similar specimen stage assembly with some modifications. Figure 1 shows the different components of the specimen stage. The base block (A) is made of tantalum. On both sides of the stage and at one end, 99.8% alumina plates are used to insulate the electrical connections for the heater and thermocouple from the metal frame. An alumina disc (B) 1.28 cm in diameter and 0.20 cm thick placed under a molybdenum stand (C) provides bottom heat insulation. A 5 mil Pt-Pt10%Rh thermocouple protected by alumina tubing comes through a hole in the center of the molybdenum stand. The junction spot lays in a groove and is spot-welded to the stand.

The heater (D) is very much the same as D. Wang's except for bends so that both ends of the tungsten wire come out from the bottom of the Ta radiation shields (F). The molybdenum crucible (E) can be placed on the stand so that the thermocouple junction is in direct contact with the bottom of the crucible. A corrugated Ta foil disc (G) with a 2 mm diameter hole and a thin alumina disc (H) with a 3 mm diameter hole are used as top radiation and thermal shields. The top cover shield (I) is made of Ta with a 4 mm diameter hole and is held in position by screws at the corners of the metal frame. Figure 2 shows the partially assembled stage.

A constant current D.C. power source was used for manual operation. There was very little drift in temperature and by manual adjustment a constant temperature was easily maintained. The thermocouple was checked in a vacuum chamber against a calibrated optical pyrometer in the temperature range of 800 - 1100°C. The calibration of the thermocouple was verified by observing the melting of silver in the hot stage of the scanning electron microscope. In both cases, the thermocouple gave agreement better than $\pm 5^\circ\text{C}$. A heating rate of approximately 23°C/min was used to achieve the reaction temperature of 750°C in our kinetic studies.

The commercial unreacted bronze process wire used in this study had 5377 Nb filaments in a 13.5 w/o Sn bronze matrix. A Ta barrier separated the tin bronze from the copper cladding. The outside diameter of the wire was 0.0127in. After chemically cleaning the Cu surface, the wire was inserted into a clean copper tube and the assembly was then swaged down just enough to provide a tight fit between the wire

and the copper tube. Samples were cut from this swaged rod and then polished to provide a smooth surface. The last polishing step for each sample was on a 1 μm diamond paste wheel. Most of our experiments were carried out with unetched sample surfaces.

For SEM an accelerating voltage of 35 kV and beam currents of $\sim 4 \times 10^{-8}$ amps. were used. The magnification was set at $\sim 1500\times$ so that a raster of $\sim 70 \mu\text{m} \times 70 \mu\text{m}$ was obtained. The electron beam was focused on the same area throughout the experiment. When the power was turned on to achieve the desired temperature the electron beam was shifted slightly by the electric field generated by heating coils. This was easily corrected by manually adjusting the position of the sample stage.

The TV scanning mode was normally used to observe the growth of voids. The image was recorded on a video tape recorder (VTR) with a time lapse mode. A date-time generator was added to the VTR system. The magnification of the SEM was determined by direct measurement of the cross section of filaments from the micrographs and calibrated with the reported value. The volume fraction of voids was determined from the area ratio of voids measured from micrographs.

OBSERVATION AND DISCUSSION

The polished unreacted samples were inspected by an optical microscope (magnification ~ 50 to $1000\times$), a scanning electron microscope fitted with a hot stage (magnification ~ 1000 to $3000\times$) and a scanning electron microscope equipped with EDX (magnification

~ 1000 to $10,000 \times$). No voids were observed in the unreacted samples. This indicated that all voids were indeed produced during reaction.

Figure 3 shows a sequence of TV pictures generated from the video tape. The void areas were measured and the volume fraction of voids was plotted as a function of reaction time at a reaction temperature of 750°C (see Figure 4). It is interesting to note that the volume fraction of voids levels off as reaction time increases. The leveling off of the volume fraction of voids indicates that these voids are not a surface phenomenon nor are they due to sublimation. Successive layers of samples heated in the hot stage were subsequently removed and the new surfaces were examined, using SEM-EDX and optical microscopy, to confirm the fact that the observed porosity was indeed a bulk rather than a surface phenomenon.

It is important to note that all the voids appear to be distributed randomly at the interface of filament and matrix. As reaction time increases the volume of voids increases. This causes an uneven growth of the Nb_3Sn layer along the filament surface.

Voids not only decrease the cross section area over which the load is applied, but also act as stress concentrators. (For an isolated spherical void, the stress is increased by a factor of 2)⁶. Easton and Kroeger reported that the examination of tensile cracks revealed necking of the Nb core in the void region. These voids lead eventually to fractures.

The effect of voids on the thermal conductivity depends on the temperature. At low temperatures the voids have a lower thermal conductivity than any of the solid phases. This can impede the transfer of heat and thus produce thermal instabilities under superconducting

conditions.

There is another type of void which appears in the area between bundles of filaments. They are fairly uniformly distributed along the bundle boundary. These voids appear to be very shallow. Upon removal of the surface layer these voids are like pin holes. These voids may be due to impurities on the surfaces of individual bundles before they are put together. The effect of this type of void on the physical and mechanical properties of bronze process wire has not been determined.

SUMMARY

The manufacturing process for producing multifilamentary superconductors by the bronze process is based on the solid state diffusion of tin atoms from the bronze to the niobium-bronze interface. This preferential diffusion process is similar to the phenomenon which is usually termed the "Kirkendall" effect. This effect leads to void formation in the reacted bronze process wire. Although the occurrence of this effect in bronze process wire has been reported previously², skepticism prevails in the superconducting community. In this work, a striking confirmation of the existence of voids in reacted bronze wire has been achieved by utilizing the hot stage scanning electron microscope. We have been able not only to confirm the existence of voids but also to directly observe their growth.

The mechanical properties of filament strengthened composites also depend on the properties of the interface between filament and

matrix.⁷ Kinetic studies of diffusion processes and identification of diffusion mechanisms are essential for the development of the science of interfaces on a sound basis. These studies of the diffusional processes and mechanisms must be performed in the range of interface thickness of interest for useful composites, and often this will mean that studies should be performed within the range of thickness below 10 μm . Changes in mechanism may often occur with thicker interfaces, particularly under the restrained conditions present in a composite. The capability of achieving high temperatures and high magnifications makes the hot stage scanning electron microscope an uniquely valuable tool for studying the reaction kinetics of fiber composites.

ACKNOWLEDGEMENTS

Thanks are extended to Drs. D. S. Easton and D. M. Kroeger of Oak Ridge National Laboratory for their discussion on their findings and to Mr. John Jacobsen for his metallographic work.

This work was supported by the Division of Materials Sciences, Office of Basic Energy Sciences, U. S. Department of Energy, under contract No. W-7405-Eng-48.

REFERENCES

1. A Technical Assessment of Superconducting Magnet Development for Tokamaks and Mirrors, DOE/ET-0016 (U.S. DOE).
2. D. S. Easton and D. M. Kroeger, Applied Superconductivity Conference, Pittsburgh, PA, 1978.
3. A. D. Smigelskas and E. O. Kirkendall, Trans. Amer. Inst. Min. (Metall.) Engrs. 171, 130 (1947).
4. R. M. Fulrath, 5th Annual Scanning Electron Microscopy Symposium, Chicago, 1972.
5. D. N. K. Wang, D. J. Miller and R. M. Fulrath, Scanning Electron Microscopy 1, 777 (1978).
6. W. D. Kingery, Introduction to Ceramics, John Wiley & Sons, Inc., p. 621 (1960).
7. A. G. Metcalfe, Composite Materials 1 (1974).

FIGURE CAPTIONS

- Figure 1. The components of the specimen stage:
- (A) Ta base block; (B) Alumina insulation disc;
 - (C) Molybdenum stand with thermocouple; (D) Heater;
 - (E) Molybdenum crucible; (F) Ta radiation shield;
 - (G) Corrugated Ta foil; (H) Alumina insulation disc;
 - (I) Top cover shield.
- Figure 2. Partially assembled specimen stage.
- Figure 3. Scanning electron micrographs of bronze process wire reacted in the hot stage at 750°C.
- a) after 20 minutes
 - b) after 2 hours
 - c) after 3 1/2 hours
 - d) after 6 hours.
- Figure 4. The volume fraction of voids (%) as a function of reaction time.

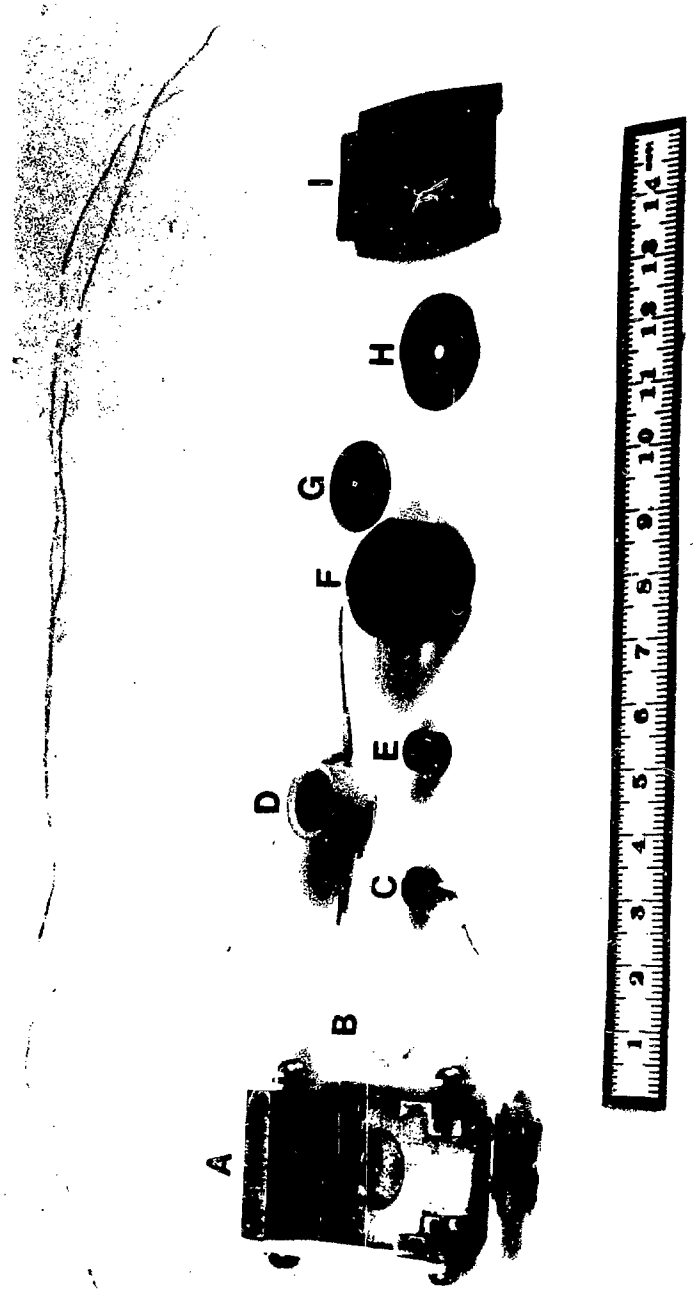
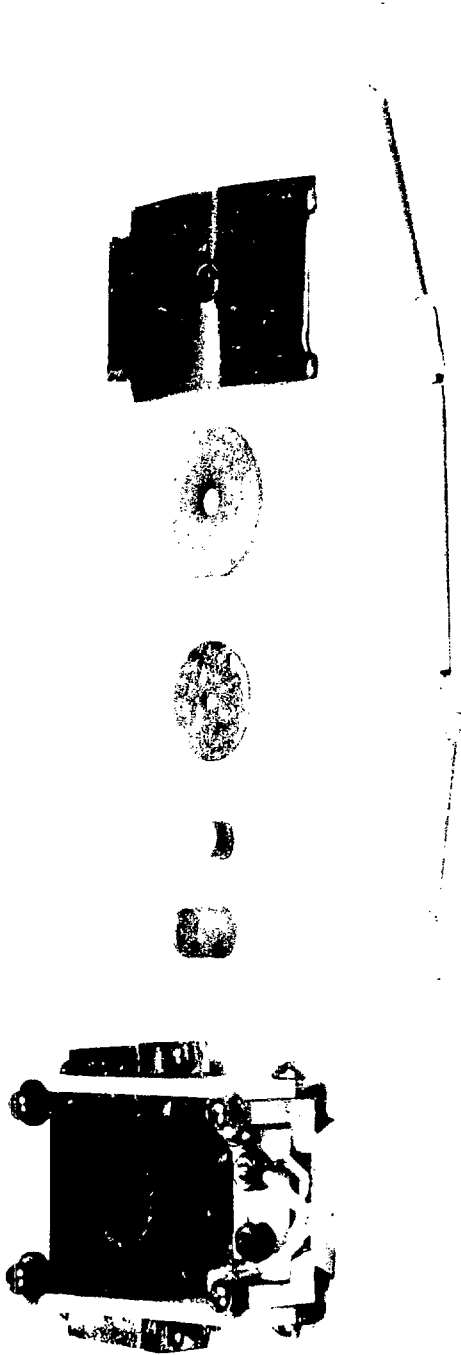


FIGURE 1.

XBB 780-13566A



XBB 780-13567

FIGURE 2.

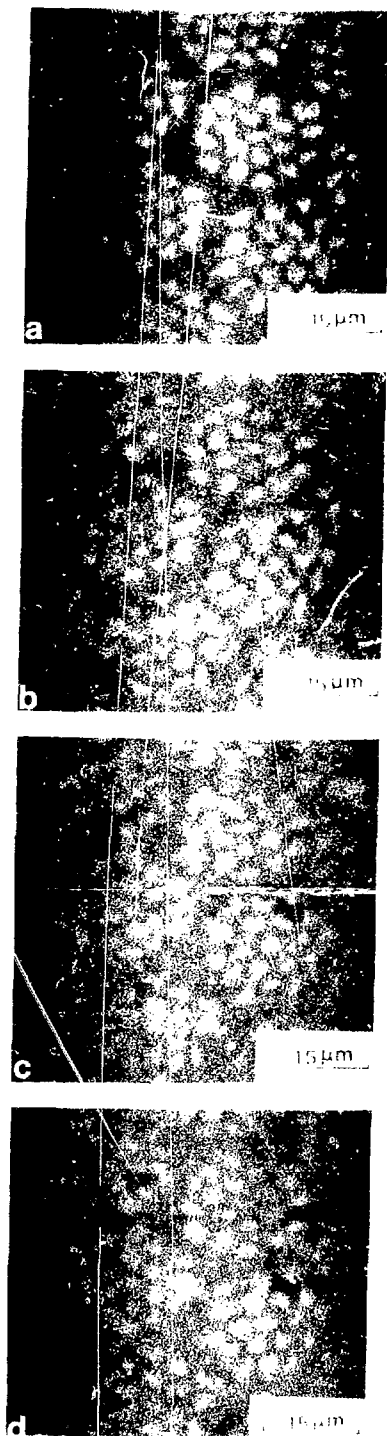


FIGURE 11

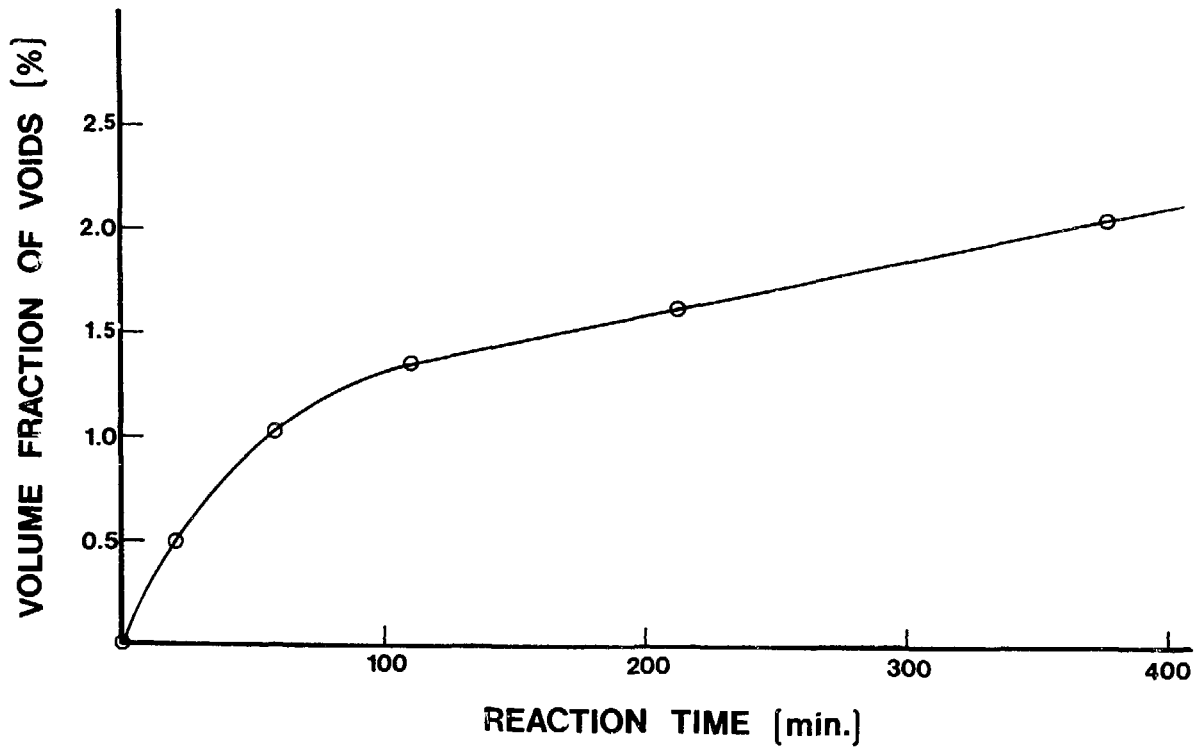


FIGURE 4.

XBL 791-7745